Clueless forms dynamic, insulin-responsive bliss particles sensitive to stress

Sheard*, K. M., Thibault-Sennett*, S. A., Sen, A., Shewmaker, F. and Cox, R. T.[#]

Department of Biochemistry and Molecular Biology

Department of Pharmacology and Molecular Therapeutics

Bethesda, MD 20814

Uniformed Services University

Short title: Clu forms insulin-responsive bliss particles

Key words: mitochondria, Clueless, Drosophila, insulin, ribonucleoprotein particle

*these authors contributed equally

[#]Address for correspondence: rachel.cox@usuhs.edu

Abstract:

Mitochondria perform a myriad of biochemical functions in the cell that integrate ATP production and metabolism. While mitochondria contain their own genome, mtDNA, it only encodes thirteen proteins required for oxidative phosphorylation, thus well over one thousand proteins required for all mitochondrial functions are encoded in the nucleus. One such protein is Drosophila Clueless (Clu), whose vertebrate homolog is Clustered mitochondria homolog (Cluh). Clu/Cluh is a ribonucleoprotein that regulates mRNAs destined for import into mitochondria and is an essential protein that regulates cellular metabolism. Clu forms large particles in the cytoplasm, although how these particles relate to nutrition and metabolic stress is unknown. Using live-imaging, we show Clu particles are highly dynamic. Clu particles appear to be unique as they do not colocalize with many known cytoplasmic bodies. In addition, Clu particle formation is highly dependent on diet as ovaries from starved females no longer contain Clu particles although Clu protein levels remain the same and insulin is necessary and sufficient for Clu particle formation. Oxidative stress also disperses particle. Since Clu particles are only present under optimal conditions we are naming them bliss particles. These observations identify Clu particles as unique, stress-sensitive cytoplasmic ribonucleoprotein particles whose absence corresponds with altered mitochondrial function and localization.

Introduction:

Mitochondria supply the vast majority of ATP to tissues. This is particularly important for high-energy tissues such as heart, skeletal muscle and the nervous system. Mutations in either mitochondrial DNA (mtDNA) or nuclear genes required for mitochondrial pathways can cause mitochondrial diseases that tend to affect these tissue types (Suomalainen and Battersby, 2018). Metazoan mtDNA encodes the same thirteen proteins, 2 rRNAs and 22 tRNAs, but this small number of products must be supplemented by over 1,000 products encoded in the nucleus (Area-Gomez and Schon, 2014). These nuclear proteins are targeted and imported into the organelle for use. How these proteins are regulated, targeted and the effect of their loss is only understood for a subset of proteins.

One such nuclear protein required for mitochondrial function is Clueless (Clu). Clu encodes a large multi-domain protein that is directly involved in regulating mitochondrial function, although many details are still not well understood (Cox and Spradling, 2009). Loss of *clu* in Drosophila is adult lethal. In uncrowded conditions, larvae are able to pupate after a short developmental delay, but the adults die after 4-7 days and look sickly immediately following eclosion (Sen and Cox, 2016; Sen et al., 2013). ATP levels are normal in larvae however levels are greatly decreased in adults who accumulate mitochondrial oxidative damage (Sen et al., 2013). *clu* mutants are male and female sterile and mitochondria are clumped and mislocalized in female germ cells, which contain damaged, swollen mitochondria (Cox and Spradling, 2009). Drosophila Clu also physically and genetically interacts with the PINK1/Parkin mitophagy complex and thus may play a role as a sensor linking mitochondrial function with destruction (Sen et al., 2015). In mice, loss of Cluh is embryonic lethal (Schatton et al., 2017). Conditional knockdown in the liver causes a metabolic disruption in hepatocytes and mitochondrial mislocalization, leading to the pups dying on post-natal day 1. Mitochondria in the hepatocytes are depleted of key enzymes used in catabolic energy pathways (Schatton et al., 2017). Altered metabolism is also found in HeLa cells with CRISPR/Cas9 deleted Cluh, as well as mitochondrial mislocalization (Wakim et al., 2017). In addition, comparison of human mesenchymal stem cells derived from umbilical cords of preterm and term newborns showed changes between the two in the mitochondrial network, as well as concurrent metabolic changes in response to an oxygen-rich environment, these differences are regulated by Cluh (Ravera et al., 2018). Clu's role in regulating mitochondrial function and metabolism is due to its role in mRNA

regulation. Clu, Cluh and yeast Clu1p are ribonucleoproteins (RNPs) (Gao et al., 2014; Schatton et al., 2017; Sen and Cox, 2016). Cluh binds and regulates mRNAs encoding proteins that will be imported into mitochondria (Gao et al., 2014; Schatton et al., 2017). Clu and Clu1p bind mRNA in Drosophila and yeast, respectively, and Clu was shown in Drosophila to associate with the ribosome, potentially at the mitochondrial outer membrane (Sen and Cox, 2016). All of these observations underscore Clu's fundamental role in regulating mitochondrial function and mitochondrial protein levels through its role as a ribonucleoprotein.

While molecular analysis has clearly demonstrated Clu is an RNP, Clu also has a characteristic subcellular pattern and it is not currently clear how this relates to its function as an RNP. Clu forms large particles in Drosophila female germ cells that are closely juxtaposed with mitochondria (Cox and Spradling, 2009). Particles are not confined to germ cells and can be found in larval neuroblasts and other neuronal cell types, somatic follicle cells in the ovary and larval muscle (Sen et al., 2013; Wang et al., 2016). Cluh also forms particles, as well as the Arabidopsis thaliana homolog, *friendly mitochondria* (*FMT*), which like Drosophila Clu is found in close proximity to mitochondria (El Zawily et al., 2014; Gao et al., 2014; Wakim et al., 2017). How the particles relate to mitochondrial function, and how they change with metabolic or nutritional changes is not known. Cytoplasmic particles are numerous, and the Drosophila female germ line has historically been an excellent tissue in which to study their function and dynamics.

Here, we examine the dynamic control of Clu particle formation and disaggregation to show Clu forms a unique and highly stress-sensitive cytoplasmic particle. Live-imaging shows Clu particles are highly dynamic and require an intact microtubule cytoskeleton in order to move processively. The oocyte does not contain particles and has very low levels of Clu protein. Clu particles do not colocalize with other well described cytoplasmic components, thus we believe these particles are unique. Yeast Clu1p also forms particles, and *clu1* deletion causes decreased growth on a non-fermentable carbon source. In addition, Clu particles are highly sensitive to nutrition and insulin. Starved follicles no longer have particles in germ cells and surrounding somatic follicle cells, even though Clu protein levels remain the same. This effect is likely due in part to insulin signaling, as insulin is both necessary and sufficient for particle formation. Nutritional stress is not the only particle disruptor, as increased mitochondrial oxidation also causes particles to disperse. Because Clu particles are unique, and in contrast to stress granules and processing bodies that disperse with stress, we are naming

them bliss particles. Finally, we show mitochondrial localization in germ cells is completely dependent on stress-free conditions, as any of the aforementioned stressors cause clumping and mislocalization. These observations shed light on how Clu's subcellular localization is related to its ability to regulate metabolism.

Results:

Clu particles are abundant and highly dynamic

Clu protein is highly abundant and forms particles in the cytoplasm of many cell types. Female germ cells have been an excellent tissue in which to study Clu particles as they are highly metabolically active, are very large and have a large number of particles (Kato and Nakamura, 2012). In order to better understand Clu's role in the cell, we used live-imaging to dissect Clu particle dynamics and whether it recapitulates our previous observations in fixed tissues (Cox and Spradling, 2009; Sen et al., 2015). To do this, we imaged Clu-GFP in the GFP trap line *clueless*^{CA06604} (Buszczak et al., 2007). Clu particles are even more abundant using live-imaging compared to fixed tissues (Supp. video 1). This may be due to the smaller particles being washed out during fixation, as well as particle movement making is easier to distinguish smaller particles from background. As with many cytoplasmic bodies and ribonucleoprotein particles, particularly in Drosophila female germ cells, Clu shows a mix of stochastic and directed movement. At any given time, approximately 10% of the particles appear to be moving in a processive and directed manner over the course of 50 seconds (Fig. 1A-A″, yellow arrows, Supp. video 1). For particles that move quickly, kymographic analysis supports that the movement is microtubule based (Fig. 1B, C) (Liao et al., 2017). Adding the microtubule destabilizer colcemide causes particles and mitochondria to remain completely stationary, as well as disrupts the microtubule cytoskeleton as expected (Supp. videos 2, 3, 4, Fig. S1). The dynamics of the particles (percentage in motion at any given time, speed and switching between phases of directed motion and becoming stationary) is very similar to observed mitochondrial motion (Liao et al., 2017). The rest of the particles under normal conditions are either fairly stationary or appear to move with the bulk cytoplasmic movement driven by the microtubule cytoskeleton. As with fixed tissue, abundant Clu particles are present in the surrounding somatic follicle cells, but do not appear to move as much, likely due to the restrictive size of the cells (Fig. 1D, Supp. video 5). In addition, Clu protein levels are very low in the oocyte relative to the nurse cells, and we never observe Clu particles in the oocyte

(Fig. 1E). This may be due to the metabolic differences between the oocyte and nurse cells, with the oocyte relatively quiescent and the nurse cells very metabolically active. It also suggests that Clu is not moving into the oocyte from the nurse cells during follicle development, or that it is actively degraded in the oocyte during these stages. In addition, with our fixed tissue and antibody labeling, it was not completely clear how great of a contribution the "background" Clu played. With the live-images, it appears that Clu particles comprise the overwhelming amount of visible protein.

Clu particles do not colocalize with many known structures

Lack of Clu causes mitochondrial deficits in all tissues examined. Since Clu interacts with several proteins on the mitochondrial outer membrane and human homolog Cluh binds mRNAs destined for mitochondrial protein import, these deficits are clearly a direct effect of protein loss (Gao et al., 2014; Sen and Cox, 2016; Sen et al., 2015). As we have previously shown, Clu particles tightly associate, but do not co-localize, with mitochondria (Fig. 2A)(Cox and Spradling, 2009). Using structured illumination microscopy to get slightly better resolution, the particles appear less amorphous compared to traditional confocal microscopy (Fig. 2A, inset). As noted, while every large particle that is seen in fixed tissues associates with several mitochondria, there are clearly many more mitochondria not associated with large particles. Initially, we thought this mitochondrial association may be due to Clu being involved in autophagosome formation and mitophagy. However, Clu does not co-localize with Atg8a, the LC3 homolog (Fig. 2B). Nor does Clu co-localize with a second stress-associated cytoplasmic body, processing bodies (Fig. 2C). Finally, in Drosophila larval muscle, it appeared that Clu associated with ER-exit sites (Wang et al., 2015). However, in female germ cells and surrounding follicle cells we do not observe any co-localization with components of the secretory pathway. Clu particles do not show any particular association with endoplasmic reticulum (Fig. 2D). In addition, in the follicle cells Clu particles are distinct from ER exit sites/COPII vesicles (Fig. 2E), cis Golgi (Fig. 2F) and trans Golgi (Fig. 2G). Therefore, we believe Clu forms unique particles in the cytoplasm specific to mitochondrial function.

Clu particles are conserved

Clu has strong homologs in many different species, including humans, and we have demonstrated the human homolog, Cluh, fully rescues the Drosophila mutant (Sen et al., 2015). The mouse Cluh homolog was shown to share many attributes of Drosophila Clu, and a Cluh knockout mouse is embryonic lethal (Gao et al., 2014; Schatton et al., 2017). Yeast has an uncharacterized homolog, Clu1p (Fig. 3A). Clu1p was identified as a ribonucleoprotein by the Parker lab in a global screen for RNPs (Mitchell et al., 2013). The *clu1*:*CLU1-GFP* strain contains a GFP insertion at the endogenous *clu1* locus (Huh et al., 2003). Fixation and antibody labeling shows that Clu1p, similarly to Clu, is punctate in the cytoplasm and forms particles (Fig. 3B, arrows). We have previously shown Drosophila Clu sediments in heavier fractions on a sucrose gradient and associates with the ribosome at the mitochondrial outer membrane (Sen and Cox, 2016). Clu shifts to lighter fractions with the addition of RNAse and EDTA. Yeast Clu1p exhibits a similar pattern on a sucrose gradient (Fig. 3C) compared to Drosophila (Fig. 7E). Since Clu directly affects mitochondrial function, we tested whether a *clu1Δ* knockout yeast strain shows defects associated with loss of mitochondrial function. Wild type yeast normally use fermentation (not oxidative phosphorylation) to produce ATP and grow well in a fermentable carbon source such as glucose (Fig. 3D). *clu1Δ* grows equally well as wild type on media containing glucose as can be seen with serial dilution (Fig. 3D). However, when grown on the non-fermentable carbon source glycerol, which forces the cells to use oxidative phosphorylation, *clu1Δ* shows decreased growth compared to wild type (Fig. 3D). This was true in two different wild type backgrounds (BY4741 and W303) and with three re-derived *clu1*::*KANMX* deletions. The poor growth and small colonies can clearly be seen after growing a small number of cells on glycerol for over a week (Fig. 3E). Petite colony formation is another commonly used assay to test for genes affecting mitochondria. Petite colonies arise due to defects in the respiratory chain and occur in mutants that are defective in oxidative phosphorylation even when grown on a fermentable carbon source. A strong mutation will give many petite colonies. Newly derived *clu1Δ* in a BY4741 background had a slightly higher percent (6.5%) petite formation vs wild type BY4741 (3.9%) when grown on YPdextrose.

Clu particles are sensitive to nutritional stress

During dissections, we have observed it was very important to have well-fed females in order to reproducibly see robust Clu particles, suggesting ample access to food was important. To analyze the effect of nutrition on Clu particle dynamics, we systematically starved and refed flies in order to determine how feeding affected particle formation. Wild type females fed wet yeast paste changed daily for 4-7 days always have robust Clu particles (Fig. 4A-A″). However, starving the same well-fattened flies for five hours on water completed abolishes particles, resulting in what appears to be slightly elevated diffuse Clu in the cytoplasm (Fig. 4B-B″). Surprisingly, re-feeding yeast paste for as little as two hours completely reverses this observation, resulting in almost pre-starvation levels of particles (Fig 4. C-C″, D). These results were the same for the surrounding somatic follicle cells (Fig. 4, E-G″). The relatively mild five-hour starvation (typical starvation in the literature lasts >24 hours (Barth et al., 2011; Nezis et al., 2009)) does not result in any behavioral defects and levels of ATP remain essentially normal, with perhaps a small increase in the starved flies presumably due to compensatory metabolic mechanisms (Figs. 4H, 7C). Importantly, particle disaggregation is not due to protein degradation as Clu protein levels remain the same from ovary extract of all three conditions (Fig. 4I, J). These results support nutrition as an important regulator of Clu particle formation, and that their formation and disaggregation are highly dynamic and reversible.

Trailerhitch (Tral) is a ribonucleoprotein that is a component of processing bodies (Barbee et al., 2006; Wilhelm et al., 2005). Under well-fed conditions, Tral forms its characteristic small particles in the cytoplasm, is concentrated in the anterior of the oocyte and is also diffusely cytoplasmic (Fig. 5A′) (Wilhelm et al., 2005). In the same follicle, Clu forms large particles (Fig. 5A). After five-hour starvation, Tral forms very large processing bodies in the nurse cells and oocyte which capture all the diffuse cytoplasmic staining causing a reduction in "background" intensity (Fig. 5B′, B″, C) (Burn et al., 2015). In contrast, in the same follicle Clu particles disperse completely with an apparent rise in diffuse cytoplasmic label (Fig. 5B, B″). These observations support that Clu particles are uniquely different from particles that form in response to nutritional stress, such as stress granules and processing bodies.

Insulin is necessary and sufficient to induce Clu particle formation

Given our results that access to yeast paste has a profound, unique effect on Clu particle formation, we examined the insulin signaling pathway to determine whether this pathway was responsible for our observations. To do this, we utilized live-imaging to manipulate insulin concentration in the media. An effective media to image follicle maturation live was developed by the Montell laboratory (Prasad et al., 2007). This media is based on Schneider's media and has additional insulin (see materials and methods). Imaging follicles from *clueless*^{CA06604} females reared on standard food alone and dissected in media without insulin results in approximately 20% of the follicles containing Clu particles (Fig. 6B). This is similar to the number found after five-hour starvation using this assay (Fig. 6B), and both are slightly higher than dissecting in Grace's using our standard protocol, followed by fixation (Fig. 4D). Dissecting in media without insulin, then adding insulin while imaging resulted in robust Clu particle formation within ten minutes of insulin addition (Fig. 6, A-A'", Supp. video 6). This method gave greater than 80% of the follicles containing Clu particles (Fig. 6B), which is similar to what we find using fixation and well-fed females (Fig. 4D). The live-imaging result upon insulin addition was similar whether the females were starved on water or standard food (Fig. 6B). While 200ug/mL is the standard concentration, for this assay we found 100 or 50 ug/mL did not give dramatically reduced percent follicles containing Clu particles. These results support that insulin is sufficient to induce particle formation.

To further assess the role of insulin in Clu particle regulation, we used clonal analysis to increase and decrease signaling in the surrounding somatic follicle cells. In control FRT82B clones, particles are present in both GFP+ and GFP- sibling clones (Fig. 6C, C'). To increase insulin signaling, we made clones mutant for *TSC1*, a negative regulator of insulin signaling. *TSC1* mutant clones gave the same result as the control, namely mutant GFP- clones contained particles as well as the wild type control GFP+ clones (Fig. 6D, D'). The particles may be larger and more plentiful with this increased signaling, but this was difficult to quantitate. To determine the effect of lack of insulin signaling has on Clu particle formation, we made mutant follicle cell clones of *InR* using two alleles, *InR*^{399} and *InR*^{E19}. Loss of *InR* resulted in a loss of Clu particles in the mutant clones compared to wild type sibling clones (Fig. 6E, E'). These results support that increasing insulin signaling has

no effect on Clu particle formation, and loss of insulin signaling causes loss of particles, indicating insulin is required for particle formation.

Clu particle formation is sensitive to mitochondrial oxidative stress

Nutritional stress and lack of insulin causes particles to disaggregate. While the insulin signaling result is specific, the downstream effects on the cell are a generalized stress. In order to determine the effect different stress has on Clu particle formation, we examine mitochondrial oxidative stress, examining *Superoxide Dismutase 2* (*SOD2*) mutants. SOD2 is a mitochondrial protein responsible for scavenging free radicals inside the organelle (Fridovich, 1995). Loss of SOD2 causes an increase in mitochondrial oxidation (Kirby et al., 2002; Sen et al., 2013,Paul, 2007 #95). The protein does not appear to be required for embryogenesis or larval development but is crucial for adults that are much higher users of oxidative phosphorylation compared to the earlier stages of development. *SOD2* mutant flies eclose at normal numbers and appear relatively healthy at first, but quickly deteriorate and die within 24 hours (Paul et al., 2007; Sen et al., 2013). Before that, their ovaries develop normally, however, they completely lack Clu particles (Fig. 7B). As we have shown previously, *SOD2* mutant adults have low levels of ATP (Fig. 7C) (Sen et al., 2013), but Clu levels are not reduced and may be slightly increased (Fig. 7D). We have previously shown Clu sediments in the heaviest fractions on a sucrose gradient, and these fractions can be shifter lighter with the addition of RNAse or EDTA (Sen and Cox, 2016). Examining sedimentation of Clu in *SOD2* mutants vs. *SOD2*/+ control, we see there is a shift to the lighter fractions as well. This could be related to lack of Clu particles, or to a change in Clu's role as a ribonucleoprotein or its role in binding the ribosome. To determine the effect of oxidation of particle stability using live-imaging, we added H_20_2 to the insulin-containing culture media of follicles dissected from *clueless*^{CA06604} well-fed females. Particles started to disaggregate in as quickly as five minutes after addition of H_20_2 indicating general oxidative stress is also effective (Fig 7. F-F", Supp. video 7).

Mitochondrial mislocalization in Drosophila female germ cells is downstream of stress

We have shown mitochondria mislocalize in female germ cells due to a variety of mitochondrial dysfunction, including loss of *clu*, *PINK1* and *parkin* (Cox and Spradling, 2009; Sen et al., 2015). In order to determine how

generalized this phenomenon is, we examined mitochondrial localization under the various stressors we examined for Clu particle formation. Under well-fed conditions, mitochondria are always reproducibly and stereotypically evenly dispersed in developing follicles in the ovary, as previously described (Fig. 8A) (Cox and Spradling, 2003). However, after five-hour starvation, mitochondria form clumps in the nurse cell cytoplasm, reminiscent of *clu* mutants (Fig. 8B, arrow, F). After only two hours re-feeding on yeast paste, mitochondria again become evenly dispersed throughout the nurse cell cytoplasm and are back to the well-fed pattern (Fig. 8C). *SOD2* mutants show a very similar pattern of mitochondrial mislocalization (Fig. 8E, arrow). To use live-imaging, we dissected well-fed *clueless*^{CA06604} female follicles and added TMRE (tetramethylrhodamine ethyl ester) to visualize mitochondria, and H_20_2 to induce oxidative stress. TMRE is a cell-permeant cationic dye that preferentially sequesters in mitochondria with high membrane potential. When the mitochondrial membrane potential is lost, the organelle no longer retains the dye and becomes dimmer. At time zero, in well-fed follicles, TMRE-labeled mitochondria are evenly distributed throughout the nurse cell cytoplasm (Fig. 8G, Supp. video 8). Once the follicles incubate in H_20_2 for approximately five minutes, mitochondria already start to clump and aggregate in the cytoplasm (Fig. 8G'). After ten minutes, oxidative damage is to the point where most mitochondria are quite dim, with only a small subset still fluorescing (Fig. 8G"). These results indicate that under well-fed optimal conditions, mitochondria in female germ cells should be evenly distributed throughout the cytoplasm. Once the cells undergo stress, whether from oxidative damage, nutritional stress, or mutation, mitochondria no longer retain their normal location. This effect occurs quite quickly, and with respect to nutrition, can be readily reversed.

Discussion

Here we show that Clu particles, which we have named bliss particles, are highly dynamic cytoplasmic bodies whose formation and dispersal is highly dependent on stress. Clu bliss particles tightly associate with mitochondria, but do not co-localize with many other cellular components, including endoplasmic reticulum and components of the Golgi apparatus (Fig. 2). This supports that they are a new cytoplasmic particle, which would be the first one identified that specifically supports mitochondrial function. Initially, we thought Clu particle mitochondrial association was targeting damaged mitochondria for destruction. However, this does not

appear to be the case as there is no localization with Atg8a, a marker for autophagosomes, which engulf damaged mitochondria during mitophagy. In addition, conditions that would be expected to increase mitophagy, such as loss of *SOD2*, do not increase the number of particles (Fig. 7). Furthermore, Clu particles have the opposite response to starvation stress as Trailerhitch, a component of processing bodies. The dynamic movement of particles in the germ cells is very similar to other ribonucleoprotein particles, and the particles that undergo directed processive movement do so at a speed consistent with mitochondrial movement. The directed movement appears to rely on the microtubule cytoskeleton, as disruption from colcemide treatment causes all particles to become stationary. We have observed several mutant situations where Clu particles are lacking, including loss of *PINK1*, *parkin* and *SOD2*, which perhaps is not surprising given that the flies are female sterile. However, even *PINK1*;*clu* and *parkin*:*clu* transheterozygotes fail to maintain Clu particles.

A striking observation is how acutely and reversibly sensitive Clu particle formation is to nutrition. Flies reared optimally with plentiful yeast paste always have large particles, which using live-imaging are clearly even more abundant than we previous realized since fixation eliminates or masks the smaller ones. A five-hour starvation with water only, which is relatively mild, completely eliminates all particles. Re-feeding with yeast paste for only two hours completely restores the particles. Furthermore, insulin addition to cultured follicles causes particles to form in as little as ten minutes. From our live-imaging, feeding water or standard fly food without yeast paste gave similar results and a low percentage of follicles containing particles. Furthermore, either condition clearly does not adversely affect the flies as they behave normally and have normal levels of ATP. Thus, the metabolic effect of lack of yeast paste quickly regulates Clu particles and affects the metabolic state of germ cells.

Drosophila Clu and vertebrate Cluh are ribonucleoproteins, and Cluh was shown to preferentially bind mRNAs encoding nucleus-encoded mitochondrial proteins. Loss of Clu/Cluh disrupts mitochondrial function by reducing ATP, mislocalizing mitochondria, causing mitochondrial ultrastructural changes, and altering metabolism. Drosophila Clu associates with the ribosome, and can do so at the mitochondrial outer membrane, suggesting it may have a role in site-specific or co-translation protein import. We do not yet know if Clu particles are the sites of translation for Clu-bound mRNAs, or whether they are enriched with mRNAs. Since there are many small Clu particles present, it is possible that a larger fraction of mitochondria is associated with

particles than we can see using fixed tissue imaging. Clu associates with several mitochondrial outer membrane proteins, including TOM20 and Porin, and also self-associates, however we still do not know exactly how and why Clu particles so tightly associate with mitochondria. Attempts to simultaneously visualize mitochondria and Clu particles live have been stymied by follicle sensitivity to TMRE addition (the Clu particles disperse) but can perhaps be accomplished in the future with fluorescently labeled mitochondria. Clu particle formation and dispersal may be important for Clu's role in controlling metabolism through regulating catabolic enzymes. Since the particles respond so quickly nutritional cues, they may represent an additional control for mRNA translation, with translation rates different in the presence and absence of particles. This hypothesis remains to be tested.

It is important to highlight the effect of various stressors on mitochondrial localization in the germ cells. Mitochondria are the proverbial "canary in the coal mine", as mitochondrial stress appears to be the first indication of general cellular stress. For example, swollen mitochondria appear before disruptions in the cytoskeleton. And clearly, not feeding female flies sufficiently not only disperses Clu particles, but also causes mitochondrial mislocalization. Properly feeding females, as well as addition of insulin to culture media if performing live-imaging, is critical to keep mitochondria in the proper location.

There have not yet been patients presenting with mitochondrial disorders identified who harbor mutations in *Cluh*. This is somewhat surprising given how large the protein is, however, it may be any perturbations in Cluh are either not compatible with life or cause very early lethality. This is supported by the mouse Cluh knockout and the observation of the difference in umbilical cord mesenchymal stem cells between preterm and term births in humans. Nonetheless, given how Clu forms dynamic cytoplasmic particles highly sensitive to stress and is an important RNP critical for directly affecting mitochondrial function and biogenesis, understanding Clu's molecular role and how its mRNA binding is related to cytoplasmic localization will be important in the future.

Materials and Methods:

Fly stocks: The following stocks were used for experiments: w^{1118}, *clueless*^{d08713}/CyO Act GFP *(Cox and Spradling, 2009), trailerhitch*^{CA06517}, *Sec61α*^{CC00735}, *clueless*^{CA06604} (Buszczak et al., 2007), *SOD2*$^{\Delta 2}$/CyO Act GFP, FRT82B, FRT82B GFP/TM3 (Bloomington Drosophila Stock Center), FRT82B *TSC1*^{Q87X}/TM3 (Tapon et al., 2001), FRT82B *InR*^{339}/TM3, FRT82B *InR*^{E19} (LaFever and Drummond-Barbosa, 2005). Flies were reared on either standard cornmeal fly media or standard cornmeal fly media supplemented with yeast paste at 22° or 25° C.

Clone generation: 0-24hr females of the appropriate genotype were fed yeast paste for 24 hr, then heat shocked 2x 1 hour in a 37°C water bath, morning and evening. Except for during heat shock, the flies were kept undisturbed on a quiet shelf at room temperature. After 24 hours feeding yeast paste, 3x ten flies were dissected in parallel with controls. Clones were distinguished by absence of GFP antibody labeling. *TSC1* mutant clones were abundant as the cells divide at a normal frequency. *InR* clones were very small and found at a very low frequency due to the shortened heat shock regimen. We found 10 clones for *InR*^{339} and 10 clones for *InR*^{E19}. Standard procedures for clone induction (3x heat shock, 7-10 days on yeast paste before dissection) gave *InR* germline clones, but did not show consistent, reproducible Clu particles for controls. Thus, the results were not interpretable, and we did not use this protocol. We assume Clu particle loss in the controls using this protocol was due to stress.

Fixed Image Immunofluorescence: Flies were collected up to 1 day after eclosion and fattened with yeast paste for 3-7 days. 60 female flies were then transferred to an empty vial containing a Kimwipe soaked in water at the bottom of the vial for five hours to induce starvation. 30 female flies continued feeding on yeast paste as controls. 30 starved flies were then transferred back to a vial with fresh fly food and yeast paste for two hours for re-feeding. 3x 10 flies were then dissected at room temperature (RT) in Grace's Insect Medium (modified) (BioWhittaker, Lonza, Cologne, Germany). Ovaries were fixed for 20 minutes in 4% paraformaldehyde and 20mM formic acid solution (Sigma) made in Grace's. Tissues were washed two times (40 minutes each) with

antibody wash buffer (1X PBS:0.1% Triton X-100:1% BSA) and were incubated in primary antibody over night at 4°C. They were then washed two times (40 minutes each) and incubated overnight at 4°C in secondary antibody. After washing, DAPI (1:1000) was added for five minutes then removed, then Vectashield (Vector Laboratories, Inc.) was added. For yeast staining, log phase Clu1p::GFP yeast grown in YPD were treated 20% paraformaldehyde to a final concentration of 4% for 20 min. The cells were spun, washed and spun twice with 1.2M sorbitol, 50mm KPOH, when resuspended in 500 uL of the same buffer. The cells were treated with zymolase for 35min at 37°C, then very carefully washed 2x with Ab wash, followed by 2 hours α-GFP sitting at room temperature with occasional gentle inversion, washed 2x with Ab wash, then added and α -rabbit Alexa-488 for 1 hour. 2x gentle wash with dapi addition in the second wash followed. The cells were then mounted in Vectashield and imaged using a Leica AF6000 Time-lapse Imaging System. The following primary antibodies were used: guinea pig anti-Clu N-terminus (1:2000) (Cox and Spradling, 2009), mouse anti-Complex V (ATP synthase (CVA)) (1:1000, Mitosciences, Inc, cat# MS507), rabbit anti-GFP (1:2000, AbCam, Catalog #Ab290), GABARAP (Atg8a) (1:200, AbCam, cat #Ab109364), Sec23 (1:500), Gmap (1:1000, DSHB), Golgin245 (1:1000, DSHB). The following secondary antibodies were used: goat anti-mouse IgG_{2b} Alexa 568 (1:500) and goat anti-guinea pig Alexa 488 (1:1000) (Molecular Probes, Invitrogen), donkey anti-guinea pig Cy3 (1:1000) and donkey anti-rabbit Alexa 488 (1:500) (Jackson Labs). Samples were imaged using a Zeiss 700 confocal microscope and 63x Plan Apo NA 1.4 lens.

Image Quantification: For Clu particle quantification, slides were scanned at 40x using a Zeiss Axio Scan.Z1 slide scanner. The number of ovarioles per slide was counted using the Cell Counter tool in ImageJ. Each ovariole on a slide was subsequently scored using the Zen blue software; an ovariole was scored as having particles if at least one follicle in the ovariole contained particles and as having no particles if no follicles contained particles. The mean percentage of ovarioles with particles in each experiment (n = 6 groups of 10 flies for well-fed group, n = 3 groups of 10 flies for starved group, n = 3 groups of 10 flies for refed group) is represented in the graph with error bars representing mean ± SD. Kymographs were generated using ImageJ from single still-frames from videos of *clueless*^{CA06604} well-fed follicles taken at 60x, with one frame captured

every second for 200 seconds. Thirty-nine particles were analyzed from 12 follicles. A representative image was used in the figure.

Live Imaging Microscopy for Drosophila Tissue Samples: *clueless*^{CA06604} females (express GFP-tagged *Clu*) that had been either fattened with yeast paste or fed only the standard cornmeal fly media, were dissected at room temperature (RT) in either Complete Schneider's Media (Schneider's *Drosophila* media [Thermofisher] with 15% Fetal Bovine Serum and 0.6X Pen-Strep solution) or Complete Schneider's Media supplemented with 200 µg/mL of insulin (insulin which did not readily dissolve in media was allowed to settle out overnight at 4°C prior to use). Ovaries were removed and further teased apart into single, isolated ovarioles. Ovarioles were then loaded onto a glass bottom 35mm dish (MatTek Corporation) and live videos were collected using a Nikon spinning disk/TIRF/3D-STORM microscope with photo-manipulation with X60 magnification at room temperature. During experiments when insulin was added to ovarioles during filming, ovarioles would be prepared as above in Complete Schneider's Media and Complete Schneider's Media containing 400 µg/mL insulin would be added to the dish with a 3mL syringe to dilute the sample 1:1, resulting in an insulin concentration of 200 µg/mL with 3 biological repeats. For Insulin response graph, flies were dissected in C.S. containing the amount of insulin indicated and viewed on Nikon spinning disk microscope as described above, individual follicles were counted to either have particles (if at least one nurse cell in follicle has particles) or no particles after focusing throughout entire follicle. Mean percentage of follicles with particles in each experiment is represented in graph with SE (calculated with standard deviation/square-root(3)). The number of follicles counted varied between 16 and 62 per biological repeat with the following follicles counted per experiment:

Non-fattened flies in C.S. with 200ug/mL insulin – 16, 39 and 62;

Non-fattened flies in 100ug/mL insulin – 27, 39, and 39;

Non-fattened flies in 50ug/mL insulin – 29, 27, and 26;

Non-fattened flies in 0ug/mL insulin – 34 and 16;

Fattened flies in 200ug/mL insulin – 29 and 20;

Starved flies in 0ug/mL insulin – 19 and 23;

Starved flies in 200ug/mL insulin – 29 and 26.

Colcemide treatments were performed as above with the follicles incubated in 1:100 Colcemide in Complete Schneider's Media with 200 µg/mL insulin for 3 hours at room temperature before imaging. TMRE was used at a concentration of 1:10,000 and treated for 20 minutes, follicles were directly imaged with no washes. H_2O_2 experiments were performed at a concentration of 1µM and treatment lasted for 15 minutes while filming.

Yeast Growth Assays: For percent petite colony formation, approximately 500 cells were plated on YPD. Normal (rho+) and petite (rho-) colonies were counted in two square regions of interest. For BY4741 wild type background: 483 rho+ out of 495 yeast cells (97.6%) and for BY4741 *clu1Δ* (newly made): 506 rho+ out of 584 cells (86.6%). For the glycerol growth assay, log-phase BY4741 wild type and *clu1Δ* strains were grown overnight in YPGlucose, then diluted the next morning and grown until achieving log-phase. The cells were then serially diluted on both YPglucose agar and YPglycerol agar and grown overnight. To image individual colonies, BY4741 wild type and *clu1Δ* strains were grown overnight in YPGlucose, then diluted an grown the next morning until log-phase. Approximately the same number of cells was spotted on YPglycerol and allowed to grow for a week before imaging.

ATP Assays: Flies were collected up to 1 day after eclosion and fattened with yeast paste for 3-7 days. 30 female flies were then transferred to an empty vial containing a Kimwipe soaked in water at the bottom of the vial for five hours to induce starvation. 15 female flies continued feeding on yeast paste as control. 15 starved flies were then transferred back to a vial with fresh fly food and yeast paste for two hours for re-feeding. Flies were then homogenized in extraction buffer (100 mM Tris-Cl, pH 8.0, 4 mM EDTA, pH 8.0; 6 M guanidine hydrochloride) (3 groups of 5 flies/50 µL extraction buffer), boiled for 4 minutes, then centrifuged at 8000 g for 5 minutes at RT. The protein concentration of the samples was determined using a Bradford assay. The ATP concentration was determined using an ATP Determination Kit (Molecular Probes, Invitrogen) according to the manufacturer's directions. 100 ml assays were performed in a 96 well plate and the luminescence was measured using a Biotek Synergy H1 luminometer. Each sample was read in triplicate. The amount of ATP was normalized against protein concentration.

Western blotting: Flies were collected up to 1 day after eclosion and fattened with yeast paste for 3-7 days. 30 female flies were then transferred to an empty vial containing a Kimwipe soaked in water at the bottom of the vial for five hours to induce starvation. 15 female flies continued feeding on yeast paste as control. 15 starved flies were then transferred back to a vial with fresh fly food and yeast paste for two hours for re-feeding. Flies were then dissected at room temperature (RT) in Grace's Insect Medium (modified) (BioWhittaker, Lonza, Cologne, Germany). Ovaries were homogenized in 150 uL of sample buffer and proteins were separated on 4-20% polyacrylamide gels using a standard SDS-PAGE protocol for Western blotting. After electrophoresis, proteins were transferred onto a Hybond-ECL nitrocellulose membrane (GE Healthsciences, Inc.) then soaked with Ponceau S for 10 min and rinsed as a further loading control. Sucrose gradients were performed as described (ref). Blots were exposed to the following antibodies: anti-Clu (1:20,000) (Cox and Spradling, 2009) and anti-α-tubulin (1:5000, Developmental Studies Hybridoma Bank, University of Iowa, Iowa City). Quantification of Western blots was performed with ImageJ, and the amount of Clu protein was normalized against α-tubulin (n = 3).

Sucrose gradients: Sucrose gradients for fly extract were performed as previously described (Sen and Cox, 2016). The modifications for yeast were the following: yeast from 5 ml YPD overnight culture was pelleted and transferred to an eppendorf tube. An equal volume of silica beads was added to the pellet plus 50ul of 1X mDXB. The tube was vortexed frequently for up to 5 minutes. 300ul 1X mDXB was added to the mixture and spun down at 2000g, twice for 5 minutes to collect the supernatant. Half the supernatant was loaded on the sucrose column.

Acknowledgements:

We would like to thank the USUHS Biomedical Instrumentation Core for imaging support and The Developmental Studies Hybridoma Bank, created by the NICHD of the NIH and maintained at The University of Iowa, Department of Biology. This work was supported by the National Institutes of Health

(1R21NS085730 to R.T.C. and 1R35GM119790-01 to F.S.) and Uniformed Services University (USUHS BIO-71-3019) to R.T.C.

Figure legends:

Figure 1. Clu live-imaging shows robust, dynamic particles in germ cells and surrounding follicle cells. (A-A″) Follicle from *clu*^{CA06604} (Clu-GFP) female. Clu particles are robust and abundant. Yellow arrow indicates example of processive movement. (B, C) A subset of particles move at speeds consistent with movement along microtubules. (B) Representative reverse image showing a single still-frame. The black line shows the orientation and plane used to make the kymograph (B). (C) Directed movement takes place between the arrows of the kymograph. Stationary phases are before and after the arrows, with the particle drifting out of focus with time. (D) Particles are also abundant in the surrounding somatic follicle cells. (E) Cross section of Clu-GFP follicle. Clu is decreased in the oocyte (white line) relative to the nurse cells and does not contain particles. Details of n values and analysis are in the materials and methods.

Figure 2. Clu particles are unique. (A) Structured illumination micrograph indicates Clu particles are granular and touching mitochondria in germ cells (inset), as previous described. (B-C) Clu particles do not co-localize with cytoplasmic bodies associated with stress such as autolysosomes (B) or Processing bodies (C) in germ cells. (D-G) Clu particles also do not appear to associate with portions of the secretory pathway. There is no overlap or particular association with ER in germ cells (D), nor with ER-exit sites (E), cis-Golgi (F) or trans-Golgi (G) in follicle cells. Green = ATP synthase (A), Atg8a (B), Trailerhitch (C) Sec61α (D), Sec23 (E), Gmap (F), and Golgin245 (G). Magenta = Clu (A-G). Scale bar: 5 μm in G for A-G, 2.5μm in A for inset.

Figure 3. Yeast Clu1p accumulates into cytoplasmic particles. (A) Cartoon diagram of the shared domain structure between Drosophila Clu (Dm) and yeast Clu1p (Sc). (B) Fixed log-phase yeast cells of strain *clu1::Clu1-GFP*. Clu1p forms puncta throughout the cytoplasm (arrows). (C) Sucrose gradient using extract from strain *clu1*::*CLU1-GFP*. Clu1p sediments in high sucrose fractions, similarly to Drosophila

Clu. (D-E) *clu1Δ* is sensitive to growth on the non-fermentable carbon source glycerol. (D) Serially diluted *clu1Δ* cultures grow normally on glucose, but not on glycerol. (E) *clu1Δ* forms small colonies after one week of growth on glycerol compared to its parental wild type strain. Green = Clu1p-GFP, blue = DAPI. Scale bar: 5 μm in A.

Figure 4. Clu particles disaggregate in response to starvation. (A-C″). Follicles from w^{1118} females. Well-fattened females fed yeast paste have many large particles in the germ cells (A). Starvation for 5 hours on H20 causes the particles to disaggregate (B). Re-feeding starved females for 2 hours with yeast paste causes Clu particles to reform (C). Quantification is shown in D. (E-G) Surrounding follicle cells show the same dynamic as the germ cells. ATP levels (H) and Clu levels (I, J) remain the same. clu^{d08713} is a positive control for low ATP levels. Details of n values are in the materials and methods. Error bars are S.E.M. Green = Clu, blue = DAPI. Scale bar: 10 μm in A for A-C" and E-G".

Figure 5. Clu particles and the Processing body component Trailerhitch respond oppositely to starvation. (A-A″) Well-fed follicles labeled with Clu and Tral. Tral shows the typical pattern of small aggregates in the nurse cells with a homogeneous background and concentration at the anterior of the oocyte (A). Upon starvation, Tral forms very large Processing bodies, as has been shown previously, and the diffuse Tral signal decreases (C). In contrast, Clu particles disaggregate and Clu becomes diffuse. Error bars are S.E.M. Green = Clu, magenta = Tral::GFP. Scale bar: 40μm in B″ for A-B″.

Figure 6. Insulin is necessary and sufficient for Clu particle formation. (A-A‴) Stills from live-image of $clu^{CA06604}$ germ cells. Females were raised on standard media (no yeast paste) and dissected in Schneider's. After addition of insulin, particles start forming in five minutes. (B) Quantification of particle formation with various concentrations of insulin. (C, E′) Clonal analysis in follicle cells. Wild type control clones have Clu particles in GFP+ and GFP- cells (C, C′). Mutant clones for *TSC1* also have Clu particles (D, D′). Mutant clones for *InR* lack particles compared to surrounding wild type sibling cells (E, E′). White = Clu::GFP (A-A‴),

green = GFP- mutant cells, magenta = GFP positive wild type siblings. n values described in materials and methods. Error bars = S.E.M. Scale bars: 20 μm in A‴ for A-A‴, 10 μm in E′ for C-E′.

Figure 7. Oxidative stress disperses Clu particles. (A, B) Clu particles are missing in *SOD2* mutant follicles (B), but present in sibling wild type females (A). (C, D) *SOD2* mutants have decreased levels of ATP compared to wild type flies, as previously shown (C), and do not have decreased levels of Clu protein (D). (E) A sucrose gradient of adult fly extract. *SOD2*/+ siblings have the characteristic Clu sedimentation pattern, with a large proportion of Clu in the heavier fractions. *SOD2* mutant flies show a shift to lighter fractions. (F-F″) Live-image stills of a well-fed $clu^{CA06604}$ follicle shows addition of H_20_2 causes particles to disperse quickly over time. Green = Clu, blue = dapi (A, B), white = Clu::GFP (F-F″). Error bars are S.E.M. Scale bar: 10μm in B for A, B.

Figure 8. Stress causes mitochondrial mislocalization in Drosophila germ cells. (A-C) Wild type flies. Well-fed females have evenly dispersed mitochondria in germ cells (A). Starvation causes mitochondria to clump (arrow) (B). Refeeding yeast paste for two hours post-starvation causes mitochondria to disperse (C). (D, E) Mitochondria in *SOD2* mutant germ cells also form clumps (arrow) compared to wild type *SOD2*/+ siblings (D). This clumping is reminiscent of loss of Clu, as previously published (F). (G- G″) Stills from live-imaging $clu^{CA06604}$. Adding H_20_2 to cause oxidative stress also causes mitochondria to clump. TMRE labeling of mitochondria indicates initially mitochondria are dispersed (G), but soon after start to clump (G′). At a later time-point, the TMRE labeling becomes spotty due to mitochondria losing their membrane potential and ability to concentrate the dye (G″). Green = ATP synthase (A-F), blue = dapi (A-F), white = TMRE (G-G″). Scale bars: 10 μm in C for A-C, 10 μm in F for D-F.

Supplemental video 1. Clu live-imaging shows robust, dynamic particles in germ cells. Follicle from $clu^{CA06604}$ (Clu-GFP) female. Imaged one frame per second for 200 seconds. Video is 34 frames per second.

Supplemental video 2. Mitochondria movement is normal without colcemide treatment. Follicle from *clu*^{CA06604} (Clu-GFP) female treated with TMRE. Imaged one frame per second for 120 seconds. Video is 34 frames per second.

Supplemental video 3. Mitochondrial movement ceases with treatment of the microtubule destabilizer colcemide. Follicle from *clu*^{CA06604} (Clu-GFP) female treated with TMRE. Imaged one frame per second for 120 seconds. Video is 34 frames per second.

Supplemental video 4. Clu particle movement ceases with treatment of the microtubule destabilizer colcemide. Follicle from *clu*^{CA06604} (Clu-GFP) female. Imaged one frame per second for 120 seconds. Video is 34 frames per second.

Supplemental figure 1. Colcemide treatment disrupts microtubules. Microtubule-GFP expressing follicles. Culturing in media shows the microtubule cytoskeleton is intact (A). Treatment with colcemide show no microtubules (B).

Supplemental video 5. Clu particles in surrounding follicle cells are more stationary than in germ cells. Follicle from *clu*^{CA06604} (Clu-GFP) female. Imaged one frame per second for 120 seconds. Video is 34 frames per second.

Supplemental video 6. Clu particle formation is induced with insulin. Follicle from *clu*^{CA06604} (Clu-GFP) female. Imaged one frame per minute for 45 minutes.

Supplemental video 7. Oxidative stress disperses Clu particles. Follicle from *clu*^{CA06604} (Clu-GFP) female. Imaged one frame per 15 seconds for 15 minutes. Video is 34 frames per second.

Supplemental video 8. Oxidative stress causes mitochondrial mislocalization in Drosophila germ cells. Follicle from *clu*^{CA06604} (Clu-GFP) female. Imaged one frame per 15 seconds for 20 minutes. Video is 34 frames per second.

References

Area-Gomez, E., and Schon, E.A. (2014). Mitochondrial genetics and disease. J Child Neurol *29*, 1208-1215.

Barbee, S.A., Estes, P.S., Cziko, A.M., Hillebrand, J., Luedeman, R.A., Coller, J.M., Johnson, N., Howlett, I.C., Geng, C., Ueda, R.*, et al.* (2006). Staufen- and FMRP-containing neuronal RNPs are structurally and functionally related to somatic P bodies. Neuron *52*, 997-1009.

Barth, J.M., Szabad, J., Hafen, E., and Kohler, K. (2011). Autophagy in Drosophila ovaries is induced by starvation and is required for oogenesis. Cell Death Differ *18*, 915-924.

Burn, K.M., Shimada, Y., Ayers, K., Vemuganti, S., Lu, F., Hudson, A.M., and Cooley, L. (2015). Somatic insulin signaling regulates a germline starvation response in Drosophila egg chambers. Dev Biol *398*, 206-217.

Buszczak, M., Paterno, S., Lighthouse, D., Bachman, J., Planck, J., Owen, S., Skora, A.D., Nystul, T.G., Ohlstein, B., Allen, A.*, et al.* (2007). The carnegie protein trap library: a versatile tool for Drosophila developmental studies. Genetics *175*, 1505-1531.

Cox, R.T., and Spradling, A.C. (2003). A Balbiani body and the fusome mediate mitochondrial inheritance during Drosophila oogenesis. Development *130*, 1579-1590.

Cox, R.T., and Spradling, A.C. (2009). Clueless, a conserved Drosophila gene required for mitochondrial subcellular localization, interacts genetically with parkin. Dis Model Mech *2*, 490-499.

El Zawily, A.M., Schwarzlander, M., Finkemeier, I., Johnston, I.G., Benamar, A., Cao, Y., Gissot, C., Meyer, A.J., Wilson, K., Datla, R.*, et al.* (2014). FRIENDLY regulates mitochondrial distribution, fusion, and quality control in Arabidopsis. Plant Physiol *166*, 808-828.

Fridovich, I. (1995). Superoxide radical and superoxide dismutases. Annu Rev Biochem *64*, 97-112.

Gao, J., Schatton, D., Martinelli, P., Hansen, H., Pla-Martin, D., Barth, E., Becker, C., Altmueller, J., Frommolt, P., Sardiello, M.*, et al.* (2014). CLUH regulates mitochondrial biogenesis by binding mRNAs of nuclear-encoded mitochondrial proteins. J Cell Biol *207*, 213-223.

Huh, W.K., Falvo, J.V., Gerke, L.C., Carroll, A.S., Howson, R.W., Weissman, J.S., and O'Shea, E.K. (2003). Global analysis of protein localization in budding yeast. Nature *425*, 686-691.

Kato, Y., and Nakamura, A. (2012). Roles of cytoplasmic RNP granules in intracellular RNA localization and translational control in the Drosophila oocyte. Dev Growth Differ *54*, 19-31.

Kirby, K., Hu, J., Hilliker, A.J., and Phillips, J.P. (2002). RNA interference-mediated silencing of Sod2 in Drosophila leads to early adult-onset mortality and elevated endogenous oxidative stress. Proc Natl Acad Sci U S A *99*, 16162-16167.

LaFever, L., and Drummond-Barbosa, D. (2005). Direct control of germline stem cell division and cyst growth by neural insulin in Drosophila. Science *309*, 1071-1073.

Liao, P.C., Tandarich, L.C., and Hollenbeck, P.J. (2017). ROS regulation of axonal mitochondrial transport is mediated by Ca2+ and JNK in Drosophila. PLoS One *12*, e0178105.

Mitchell, S.F., Jain, S., She, M., and Parker, R. (2013). Global analysis of yeast mRNPs. Nat Struct Mol Biol *20*, 127-133.

Nezis, I.P., Lamark, T., Velentzas, A.D., Rusten, T.E., Bjorkoy, G., Johansen, T., Papassideri, I.S., Stravopodis, D.J., Margaritis, L.H., Stenmark, H.*, et al.* (2009). Cell death during Drosophila melanogaster early oogenesis is mediated through autophagy. Autophagy *5*, 298-302.

Paul, A., Belton, A., Nag, S., Martin, I., Grotewiel, M.S., and Duttaroy, A. (2007). Reduced mitochondrial SOD displays mortality characteristics reminiscent of natural aging. Mech Ageing Dev *128*, 706-716.

Prasad, M., Jang, A.C., Starz-Gaiano, M., Melani, M., and Montell, D.J. (2007). A protocol for culturing Drosophila melanogaster stage 9 egg chambers for live imaging. Nat Protoc *2*, 2467-2473.

Ravera, S., Podesta, M., Sabatini, F., Fresia, C., Columbaro, M., Bruno, S., Fulcheri, E., Ramenghi, L.A., and Frassoni, F. (2018). Mesenchymal stem cells from preterm to term newborns undergo a significant switch from anaerobic glycolysis to the oxidative phosphorylation. Cell Mol Life Sci *75*, 889-903.

Schatton, D., Pla-Martin, D., Marx, M.C., Hansen, H., Mourier, A., Nemazanyy, I., Pessia, A., Zentis, P., Corona, T., Kondylis, V.*, et al.* (2017). CLUH regulates mitochondrial metabolism by controlling translation and decay of target mRNAs. J Cell Biol *216*, 675-693.

Sen, A., and Cox, R.T. (2016). Clueless is a conserved ribonucleoprotein that binds the ribosome at the mitochondrial outer membrane. Biol Open *5*, 195-203.

Sen, A., Damm, V.T., and Cox, R.T. (2013). Drosophila clueless is highly expressed in larval neuroblasts, affects mitochondrial localization and suppresses mitochondrial oxidative damage. PLoS One *8*, e54283.

Sen, A., Kalvakuri, S., Bodmer, R., and Cox, R.T. (2015). Clueless, a protein required for mitochondrial function, interacts with the PINK1-Parkin complex in Drosophila. Dis Model Mech *8*, 577-589.

Suomalainen, A., and Battersby, B.J. (2018). Mitochondrial diseases: the contribution of organelle stress responses to pathology. Nat Rev Mol Cell Biol *19*, 77-92.

Tapon, N., Ito, N., Dickson, B.J., Treisman, J.E., and Hariharan, I.K. (2001). The Drosophila tuberous sclerosis complex gene homologs restrict cell growth and cell proliferation. Cell *105*, 345-355.

Wakim, J., Goudenege, D., Perrot, R., Gueguen, N., Desquiret-Dumas, V., Chao de la Barca, J.M., Dalla Rosa, I., Manero, F., Le Mao, M., Chupin, S.*, et al.* (2017). CLUH couples mitochondrial distribution to the energetic and metabolic status. J Cell Sci *130*, 1940-1951.

Wang, Z.H., Clark, C., and Geisbrecht, E.R. (2016). Drosophila clueless is involved in Parkin-dependent mitophagy by promoting VCP-mediated Marf degradation. Hum Mol Genet *25*, 1946-1964.

Wang, Z.H., Rabouille, C., and Geisbrecht, E.R. (2015). Loss of a Clueless-dGRASP complex results in ER stress and blocks Integrin exit from the perinuclear endoplasmic reticulum in Drosophila larval muscle. Biol Open *4*, 636-648.

Wilhelm, J.E., Buszczak, M., and Sayles, S. (2005). Efficient protein trafficking requires trailer hitch, a component of a ribonucleoprotein complex localized to the ER in Drosophila. Dev Cell *9*, 675-685.

Figure 1

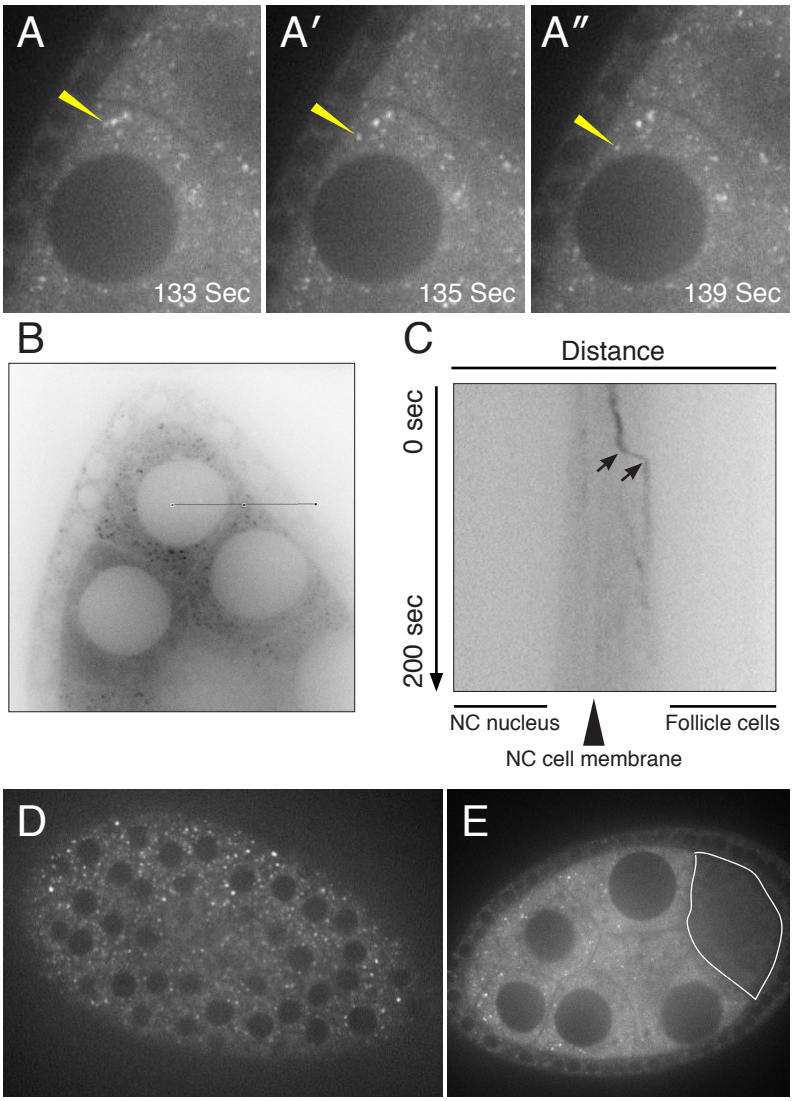
A
133 Sec
A′
135 Sec
A″
139 Sec
B
C
Distance
0 sec
200 sec
NC nucleus
Follicle cells
NC cell membrane
D
E

Figure 2

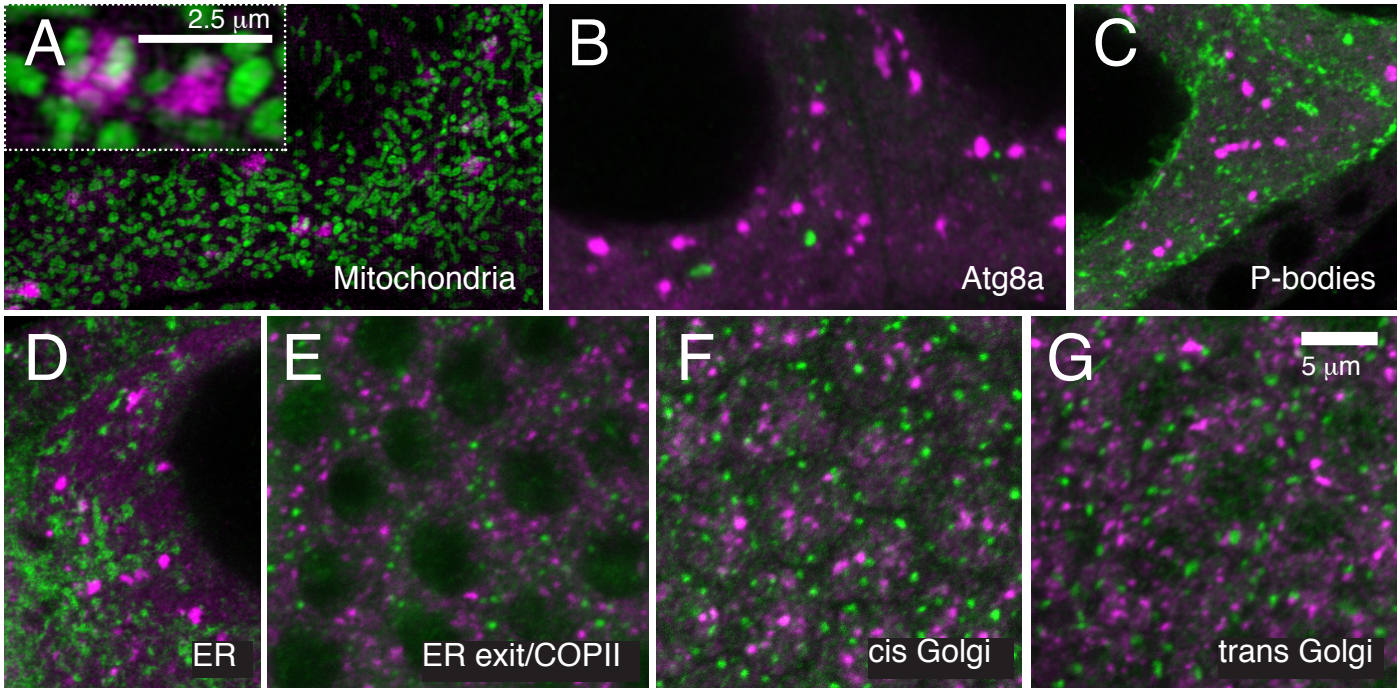
A
2.5 μm
Mitochondria
B
Atg8a
C
P-bodies
D
ER
E
ER exit/COPII
F
cis Golgi
G
5 μm
trans Golgi

Figure 3

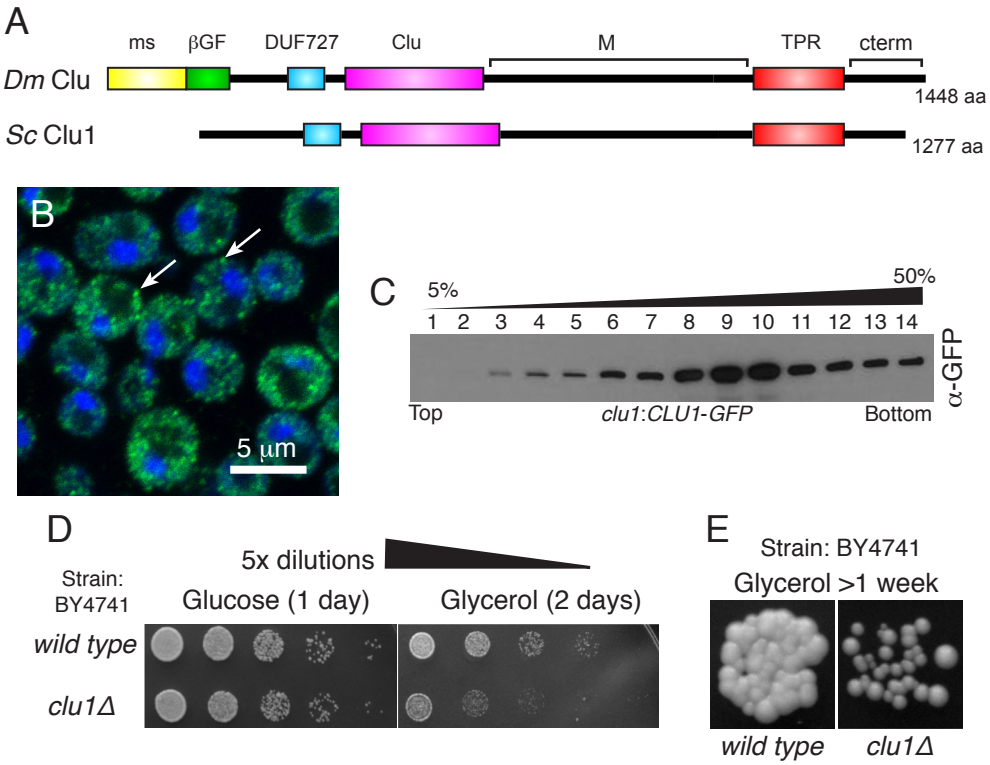
A
ms
βGF
DUF727
Clu
M
TPR
cterm
Dm Clu
1448 aa
Sc Clu1
1277 aa
B
5 μm
C
5%
50%
1 2 3 4 5 6 7 8 9 10 11 12 13 14
α-GFP
Top
clu1:CLU1-GFP
Bottom
D
Strain:
BY4741
5x dilutions
Glucose (1 day)
Glycerol (2 days)
wild type
clu1Δ
E
Strain: BY4741
Glycerol >1 week
wild type
clu1Δ

Figure 4

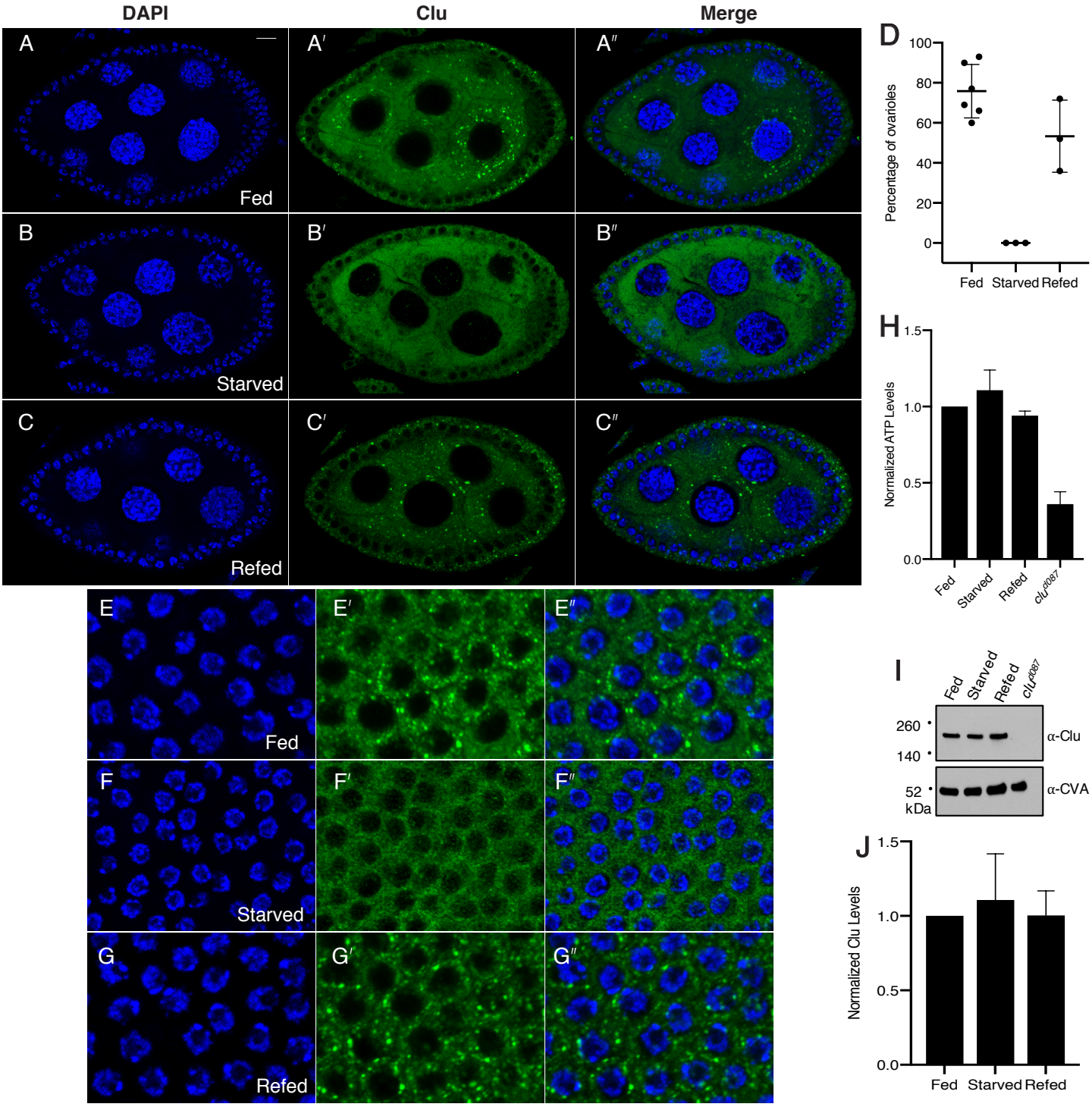
DAPI
Clu
Merge
A
A′
A″
Fed
B
B′
B″
Starved
C
C′
C″
Refed
D
Percentage of ovarioles
100
80
60
40
20
0
Fed
Starved
Refed
H
Normalized ATP Levels
1.5
1.0
0.5
0.0
Fed
Starved
Refed
clu p087
E
E′
E″
Fed
F
F′
F″
Starved
G
G′
G″
Refed
I
Fed
Starved
Refed
clu p087
260
140
52
kDa
α-Clu
α-CVA
J
Normalized Clu Levels
1.5
1.0
0.5
0.0
Fed
Starved
Refed

Figure 5

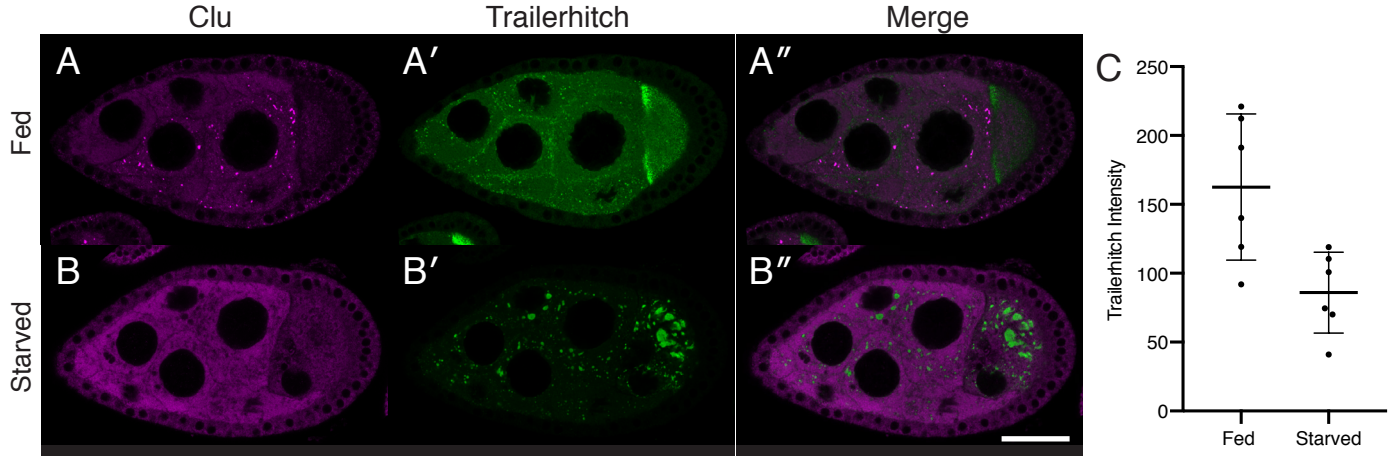
Clu
Trailerhitch
Merge
Fed
Starved
A
A′
A″
B
B′
B″
C
Trailerhitch Intensity
250
200
150
100
50
0
Fed
Starved

Figure 6

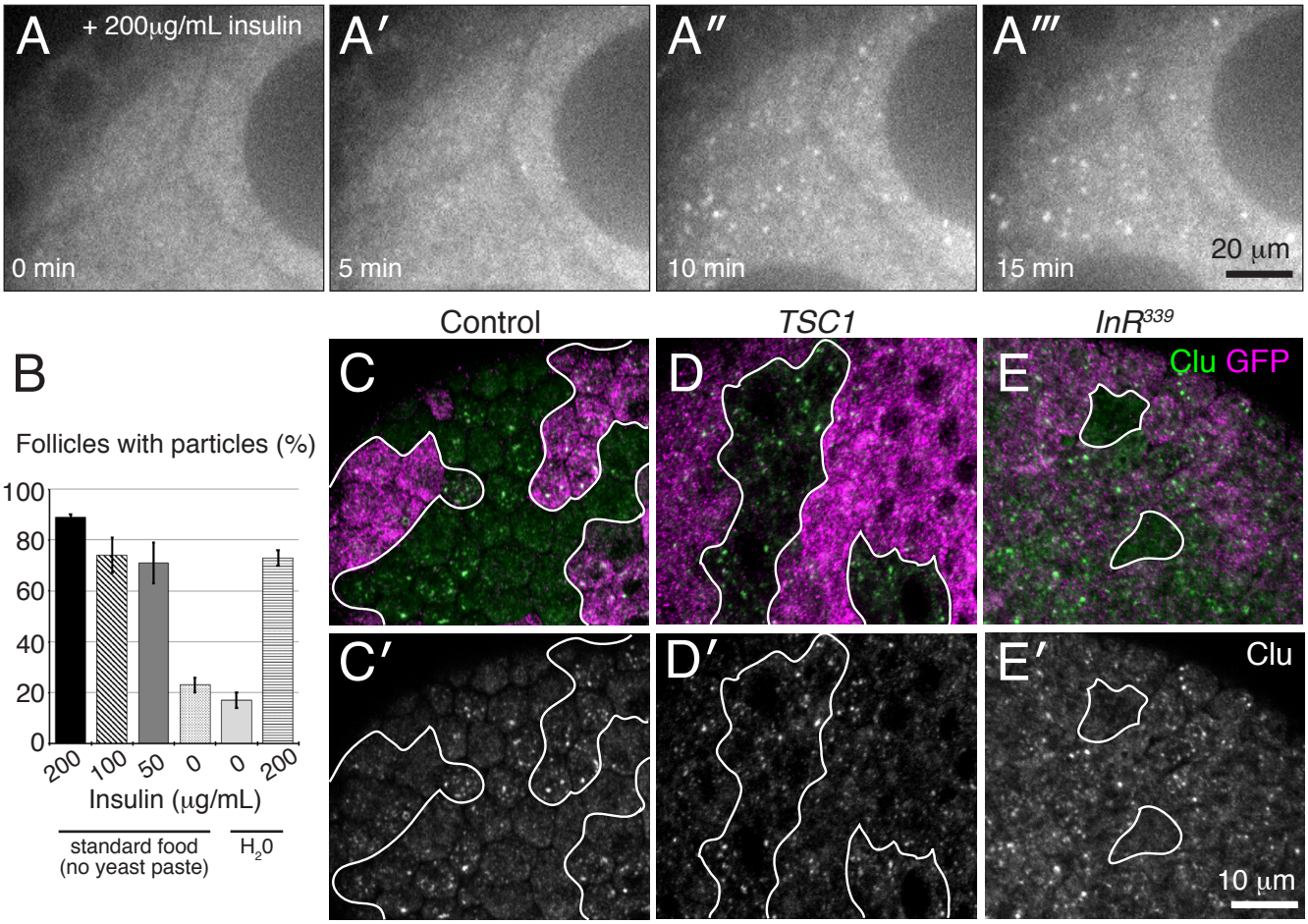
A
+ 200μg/mL insulin
0 min
A′
5 min
A″
10 min
A‴
15 min
20 μm
B
Follicles with particles (%)
100
80
60
40
20
0
200
100
50
0
0
200
Insulin (μg/mL)
standard food
(no yeast paste)
H2O
Control
TSC1
InR339
C
D
E
Clu GFP
C′
D′
E′
Clu
10 μm

Figure 7

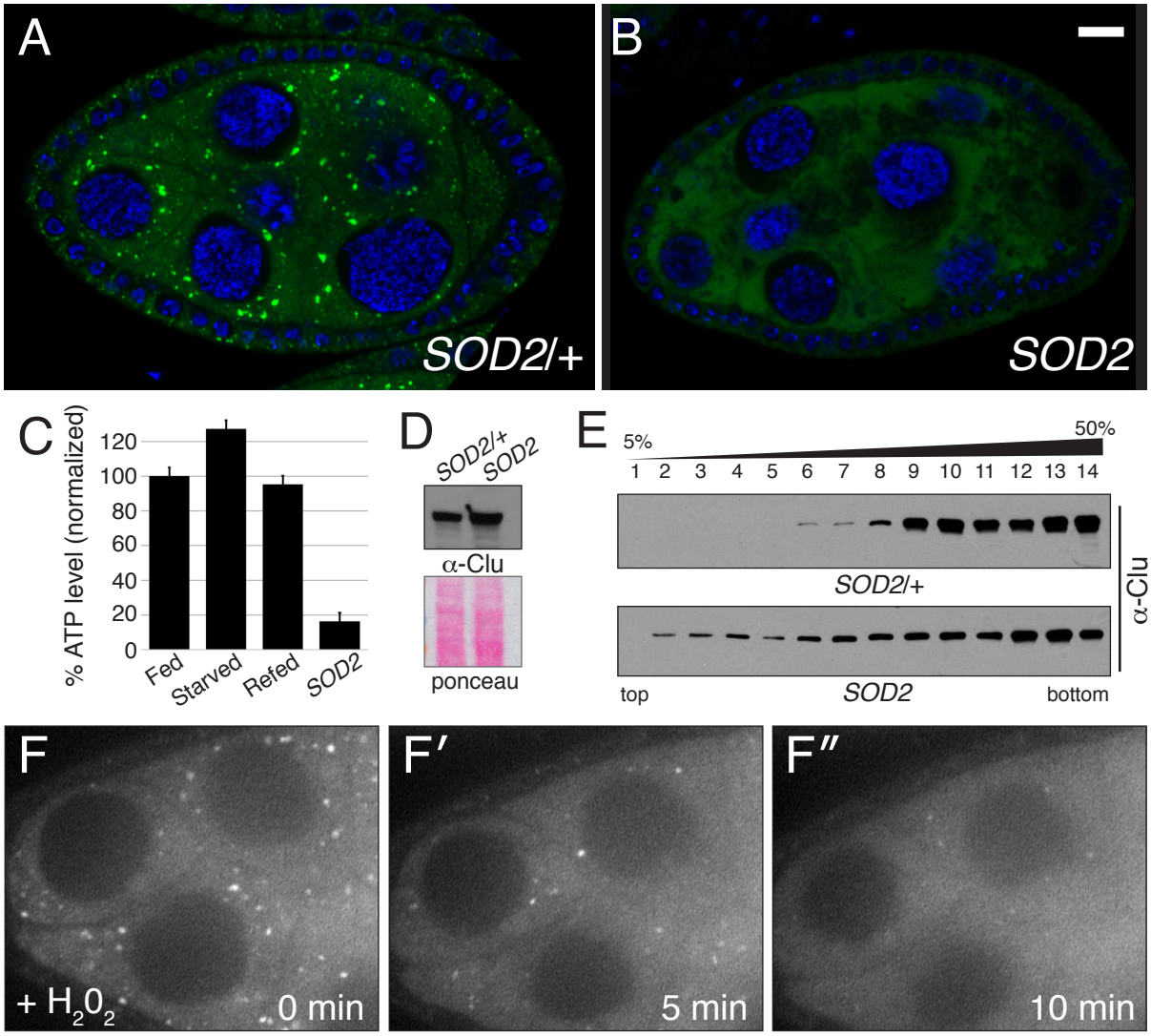
A
SOD2/+
B
SOD2
C
% ATP level (normalized)
120
100
80
60
40
20
0
Fed
Starved
Refed
SOD2
D
SOD2/+
SOD2
α-Clu
ponceau
E
5%
50%
1 2 3 4 5 6 7 8 9 10 11 12 13 14
SOD2/+
α-Clu
top
SOD2
bottom
F
+ H2O2
0 min
F′
5 min
F″
10 min

Figure 8

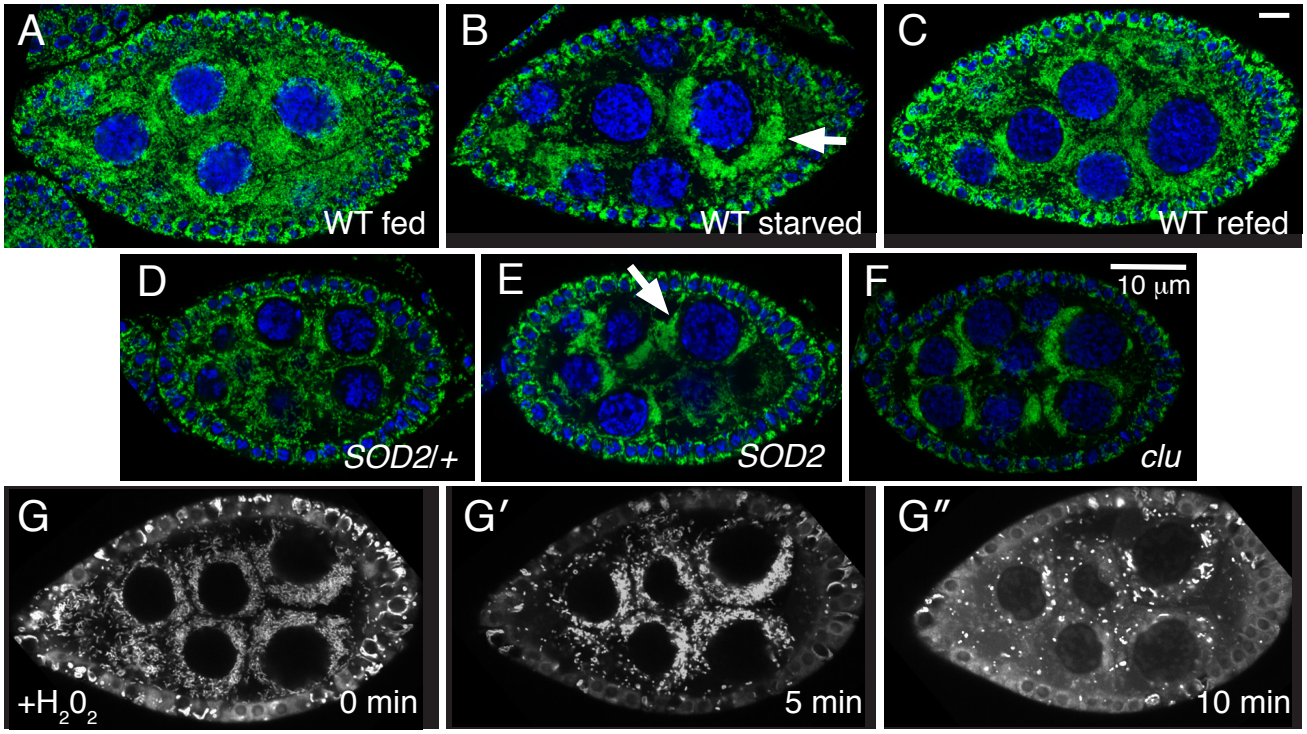
A
WT fed
B
WT starved
C
WT refed
D
SOD2/+
E
SOD2
F
10 μm
clu
G
+H2O2
0 min
G′
5 min
G″
10 min

Supp. Figure 1

Microtubule GFP

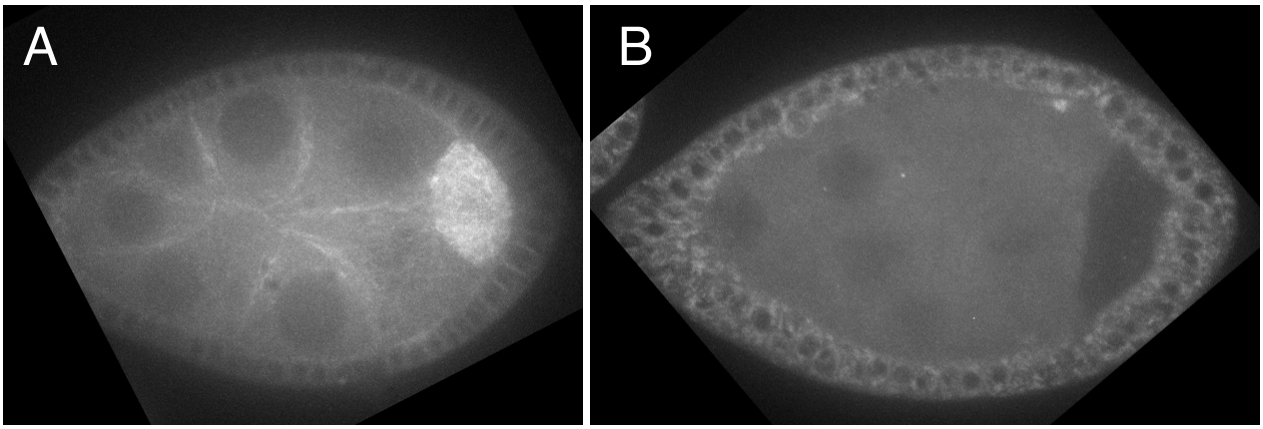

no treatment

+ colcemide